Biocompatible, biodegradable and bacteriostatic nanofiber mesh for pelvic floor repair

Preethi Arul Murugan[1] and *Jayesh Bellare*[1,2,*]

[1]Department of Chemical Engineering, Indian Institute of Technology Bombay, Powai, Mumbai, Maharashtra, India

[2]Wadhwani research center for bioengineering, Indian Institute of Technology Bombay, Powai, Mumbai, Maharashtra, India

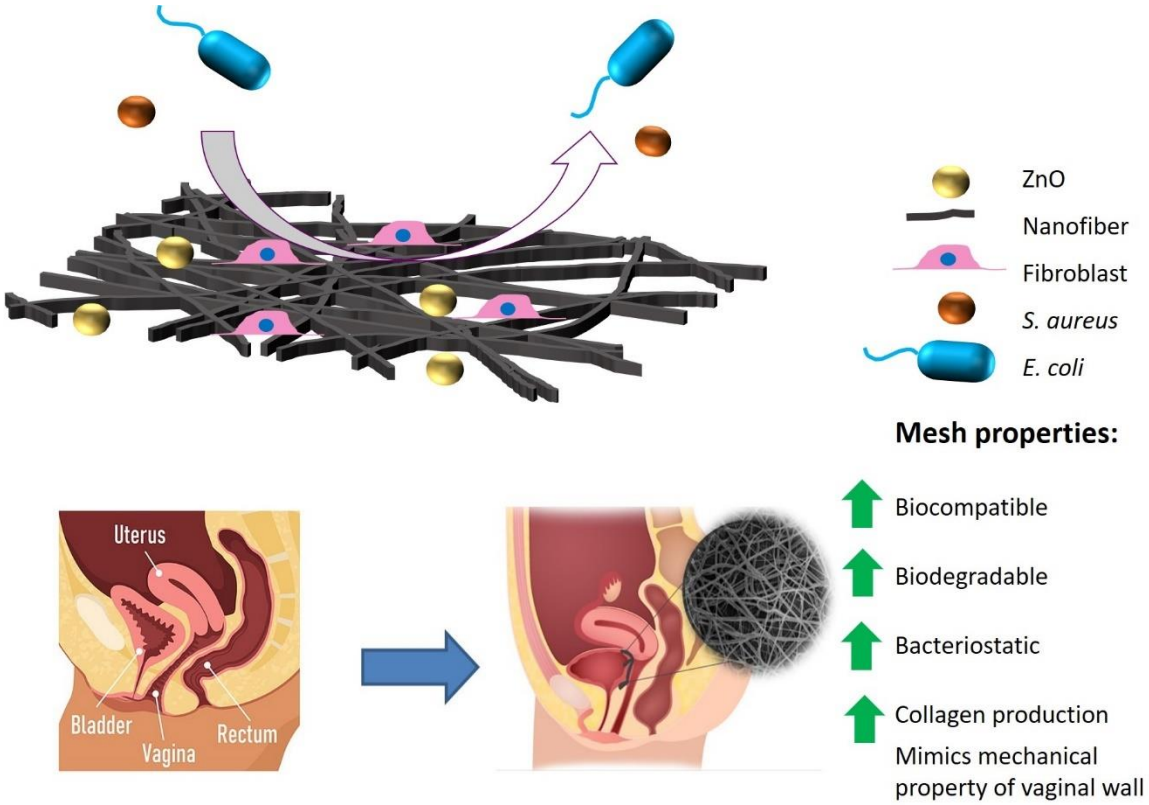

Graphical abstract

1 Introduction

The condition of descending of pelvic floor organs like uterus, bladder and/or rectum from their anatomical position towards or through vaginal opening due to loss of muscle strength that supports pelvic floor organs is called pelvic organ prolapse (POP) [1]. The prevalence of prolapse is high across the globe. As per the expert in India, 30% menopausal women have severe pelvic floor weakening. According to Continence Foundation of Australia, 1 in 5 women require medical help for prolapse [2], [3]. Similarly,

the annual rates per 1000 women of hospital admissions for POP surgery is 0.87 in Germany, 1.14 in France, and 1.13 in England [4]. Therefore, women across continents are suffering from conditions caused because of pelvic organ prolapse.

Based on the affected pelvic compartments, prolapse is majorly classified into cysctocele, rectocele and enterocele and their combinations do exist. Cystocele is the prolapse of anterior compartment leading to descending of bladder into genital hiatus. Rectocele is the prolapse of rectum into perineal body and enterocele is the prolapse of uterus or distal cervix into vaginal canal. Enterocele is the prolapse of uterus or vaginal vault through vaginal canal [5].

Treatment options vary as per the degree of prolapse (based on POP-Q system [5]). The degree of prolapse is quantified on an increasing scale from one (minor) to three (major) which may lead to complete eversion, which is a surgical emergency. For women with second and third degree prolapse, surgical correction in the form of mechanical support is required to reposition the organ in their anatomical location. Mechanical support can be provided by (i) biological grafts (autografts and allografts), (ii) xenografts and (iii) synthetic meshes. Biological grafts have advantages because they are non-immunogenic and they support tissue remodelling, but they have disadvantages like limited availability, donor site morbidity, disease transmission, etc.[6]. Therefore, there is a need for synthetic grafts that overcomes the disadvantages of biological grafts [6]. To overcome these disadvantages, non-degradable polypropylene meshes, a synthetic mesh, were widely used by direct implantation to treat POP, but they have come into disrepute recently due to surgical implantation sequelae.

The already existing non-degradable synthetic mesh that was available in the market was banned by USFDA as of April 2019, as they elicited complications like mesh exposure, organ perforation, chronic inflammation, and dyspareunia [7], [8]. Therefore, there is a need for a degradable synthetic mesh that overcomes the disadvantages of biological grafts and non-degradable synthetic mesh.

The critical factors that are involved in degradable mesh design are (i) porosity, (ii) fiber diameter, (iii) mesh density, (iv) mechanical properties (maximum load, ultimate tensile strength, strain at break and modulus) and (v) biodegradability. Porosity is

essential for nutrients and metabolites transport and host cell permeability [6]. Fiber diameter is essential for effective cell adhesion, cell fiber contact area and proliferation [9]. Mesh density modulates scar formation and mesh integration into surroundings. Patients subjected with high density nondegradable mesh had greater immunological reaction postoperatively and deterioration than lightweight mesh. This was due to "stress shielding", leading to a maladaptive remodelling response in the soft tissue characterized by loss of collagen, elastin and muscle [10]. For a degradable mesh mechanical properties should be tuned to provide sufficient strength and elasticity similar to that of vaginal tissue till tissue remodelling. The minimum mechanical property that the degradable mesh should possess are ultimate strength- 1MPa, strain 0.7 mm/mm and modulus 5MPa. These parameters were chosen based on the biomechanical property of the vaginal tissue [11]. Lastly, biodegradation in the degradable scaffold is inter linked with all the above factors. Biodegradable mesh shows less shrinkage than the nondegradable mesh in-vivo. This is because nondegradable mesh evoke immune response and inflammation [12]. Optimal but slow degradation over several months to a year will improve nutrient exchange, support host cell infiltration, adhesion and provide sufficient mechanical strength till the extra cellular matrix is laid down by the tissues.

The polymer of choice was polycaprolactone (PCL) with added polyethylene glycol (PEG) based elastomer. PCL and PEG are FDA approved (under the Generally recognized as safe category) biodegradable and biocompatible polymers. They are extensively used in tissue engineering applications for their ease in processibility and chemical modification. PCL has slow degradation rate which gives enough time for tissue to lay down the extracellular matrix (ECM) before the mesh made of PCL completely degrades and it provides stable mechanical property till ECM formation. Their mechanical property is more suitable for their application in soft tissue engineering. PEG is a water-soluble polymer has antimicrobial property. The degradability and hydrophobicity of PCL is overcome by adding PEG. In this study, PEG is functionalised with citric acid. Citric acid is a multifunctional acid, metabolic product of Krebs cycle [13], has a role in cell proliferation and metabolism [14]. Citric acid promoted collagen production in-vivo [14], which is essential for pelvic floor repair. Citric acid modified PEG imparts elasticity to the mesh and also it can undergo crosslinking during post processing such as γ-irradiation. To this

formulation we have added zinc oxide (ZnO) nanoparticles. ZnO is imparts the following properties into our mesh: addition of nanoparticles improves (i) mechanical properties [15], (ii) collagen production [16] (essential part of extracellular matrix), (iii) antibacterial properties [15] and (iv) resistant to gamma radiation [17].

The meshes for pelvic floor repairs can be made by: (i) knitting [11], (ii) 3D printing [18], (iii) solvent casting and (iv) electrospinning [19]. The choice of the manufacturing technique is based on the mechanical strength, porosity and stiffness of the materials formed out of it. Higher the fiber diameter or strut size gives higher stiffness initially thereby drop in strength. For example, Lu et al, compared and evaluated polypropylene and polylactic acid knitted mesh *in-vivo*. Before implantation, knitted mesh had ultimate tensile strength ~9 MPa. After implantation in abdominal wall of rabbit, the ultimate tensile strength dropped drastically because of inflammation till 1 month timepoint [12]. The higher the fiber diameter or strut size, higher the strain at break of mesh before implantation. After implantation, similar drop in strain at break was observed [12]. These sudden drop in material property will lead to herniation. Because of the mechanical property mismatch observed in literature, there was a need to tune the mechanical property of mesh that matches the as that of vaginal floor. In electrospinning, the fiber diameter and porosity can be fine-tuned by changing electrospinning parameters, they mimic extracellular matrix and provide better surface for cellular adhesion. Out of all fabrication techniques, electrospinning was found to be more efficient.

Therefore, in our study we chose electrospinning technique, as it supports the mesh design criteria, and it is easier to tune the mesh properties essential for effective pelvic floor repair.

2 Experimental section

2.1 Materials

Polycaprolactone (PCL, M.W. 80,000 Da), Dichloromethane (DCM), Methanol, chloroform and zinc oxide (ZnO) were purchased from Sigma-Aldrich, Mumbai, India. Polyethylene glycol (PEG, M.W. 20,000 Da), acetone and citric acid (CA) was purchased from Lobachemie, Mumbai, India. 3-(4,5-dimethylthiazol-2-yl)-2,5-diphenyltetrazolium bromide (MTT), dimethylsulfoxide (DMSO) and direct Red 80 was purchased from Sigma-Aldrich, India.

The commercial mesh was purchased from Lotus surgicals, India. Dulbecco's modified eagle's media (DMEM), sure Fetal Bovine Serum (FBS, Gamma irradiated, sterile filtered, South American) and Antibiotic Antimycotic Solution 100X Liquid (w/10,000 U Penicillin, 10 mg Streptomycin and 25 µg Amphoteric B per ml in 0.9% normal saline) was purchased from Himedia, India. GlutaMAX^{TM} (100X) was purchased from Thermofisher scientific, India. Picric Acid extrapure AR, 99.8% was purchased from SRL Pvt. Ltd. All chemicals were used as purchased.

2.2 Citric acid modified PEG (PEGC)

Citric acid modified PEG was performed through polycondensation reaction. 2:1 molar ratio of citric acid and PEG (M.W. 20,000) were heated at 160 ^{o}C and continuously stirred for 6 hrs. The pre-polymer solution is then heated at 120 ^{o}C for 24 hrs and is then cooled down to get orange coloured citric acid modified PEG (PEGC).

2.3 Electrospinning solution preparation and nanofiber fabrication

In this study we have analysed various formulations consisting of polymer PCL, additive PEGC, bacteriostatic agent ZnO, all were dissolved in a solvent consisting of chloroform, methanol mixture in 10:1 ratio to yield a solution suitable for electrospinning. The solution composition for electrospinning is PCL:PEGC= 10:1, overall polymer composition was kept at 15% and the ZnO concentration is 0, 0.1, 0.5 and 1 wt% w.r.t PCL. The solution is stirred for 1 hr and was electrospun using 10 ml syringe and blunt needle (BD Discardit^{TM} II syringe, India) in single needle electrospinning machine (ESPIN NANO, India). The electrospinning parameters were chosen based on the absence of bead on the mesh, clogging of needle during mesh fabrication. The sample codes used in this article is PCL-PEGC-y xZnO (were y= 15 and x= 0, 0.1, 0.5 and 1). The optimised electrospun parameters are given in table 1.

Table 1: Electrospinning Parameters for PCL-PEGC based micro nanofibers.

Sl.no	Sample code	Needle size (G)	Flow rate (ml/h)	Tip to collector distance (cm)	Applied voltage (KV)
1	PCL-PEGC-15	21	3	15	15
2	PCL-PEGC-15 0.1ZnO	21	3.4	15	15
3	PCL-PEGC-15 0.5ZnO	21	3.6	13	13
4	PCL-PEGC-15 1ZnO	21	3.4	15	15

2.4 Characterization

2.4.1 Scanning electron microscopy (SEM)

Electrospinning parameters were optimised using field emission gun scanning electron microscopy (JEOL JSM-7600F). All the samples were sputter coated with 10 nm thickness of platinum before analysis.

2.4.2 Tensile test

Uniaxial tensile testing of the meshes was performed using Instron 2519 series using 5 kN load cell at room temperature with a strain rate of 5 mm/min. Analysis was performed as per ASTM D882 standards. The mechanical properties consisting of ultimate load, ultimate tensile strength, strain at break and modulus were calculated from stress strain curve. Mechanical properties of meshes with respect to degradation was analysed by dipping the scaffold in phosphate buffer saline over a period of 14 and 28 days and the scaffold were washed with the help of deionised water, dried overnight and subjected to uniaxial tensile testing. Similar experiments were conducted on meshes after gamma irradiation at 25 kGy as per ISO 11137. The study is done to evaluate the effect of the mechanical properties after terminal sterilization of mesh.

2.4.3 Ion release studies

Pre-weighed meshes were immersed in 5 ml DI water at 37 ^{o}C. At predetermined time points fresh DI water is replaced with the existing DI water and DI water containing ZnO was sent for elemental analysis using inductively coupled plasma-atomic emission spectroscopy (ICPAES, make: SPECTRO Analytical Instruments GmbH, Germany, model: ARCOS, Simultaneous ICP Spectrometer).

2.4.4 Degradation studies

Pre-weighed meshes (W_i) were immersed in 2 ml DI water at 37 ^{o}C. The samples were taken out at predetermined time points, dried and weighed (W_f). \%Degradation is calculated as per the equation 1:

Equation 1: %Degradation = $(W_i - W_f)/W_f * 100$

2.4.5 Haemocompatibility Assay

Haemocompatibility assay (ASTM F756-17) is performed to access the effect of mesh performance upon contact with blood. To study haemolysis on samples, 6 ml of human blood was drawn from the antecubital arm of a healthy donor with written consent in accordance with institutional guidelines. 20 ml of whole blood of collected in two 10 ml BD Vacutainer Plus plastic plasma tubes containing sodium heparin coated anticoagulant. The heparinized whole blood was immediately centrifuged for 15 min at 1200 rpm to obtain platelet rich plasma (PRP) and packed erythrocytes.

The packed erythrocyte was washed three times using NSS (0.9% w/v NaCl), then the erythrocytes were added to 50 ml centrifuge tube and made it 50 ml using NSS to form haematocrit. Before adding haematocrit on the sample surface, samples were pre-wetted with 1 ml of NSS for 1 hour and then NSS was removed. Then, 1 ml of haematocrit and 1 ml of NSS was added on all samples (AS). 1 ml of haematocrit and 1 ml of NSS without sample was taken as negative control (AN) and 1 ml of haematocrit and 1 ml of deionized water (D. W.) was taken as positive control (AP). All the solution was incubated at 37 ^{o}C (Thermo Scientific, United Stated) for 1 h, centrifuged at 1000 rpm for 5 min and the supernatant was analysed using UV-Vis spectroscopy (Molecular devices, United States) at 542 nm. The %Haemolysis was calculated using equation 2.

Equation 2: %Haemolysis = (AS-AN)/(AP-AN) *100

2.5 In-vitro assessment of mesh

2.5.1 Cell culture condition of L929

Mouse fibroblast L929 cell line (purchased from National centre for cell science, NCCS, Pune) was cultured using DMEM media (High glucose) containing 1% GLUTAMAX^{TM}-1(100X), 1% Antibiotic and Antimycotic solution and 10% Fetal bovine Serum (FBS). The cells were maintained in a humidified incubator kept at 37 ^{o}C with 5% carbon dioxide (CO_2). For the assays, the scaffolds were placed in non-treated 24 well plate (Eppendorf USA), sterilised using 70% ethanol and UV and preconditioned using cell culture media for 1 hr each. Cells were seeded at a density of 1 x10^5 cells per cm^2 and incubated for 4 h at 37 ^{o}C with 5% CO_2. Afterwards, 0.4 ml media was added in all the wells and was replenished for every 2 days.

2.5.2 Biocompatibility assessment

MTT assay was used to evaluate the viability of cell on the mesh. MTT solution was prepared by mixing MTT with PBS at 1 mg/ml concentration and was filtered using 0.2 µm filter. After culturing cells on mesh for predetermined time points, the cell culture media was removed, and the scaffolds were washed using PBS. Then, 200 µL MTT solution was added on the mesh, which was then incubated for 4 h at 37 ^{o}C. The metabolically active cells reduce MTT in the solution into violet blue formazan crystals. The formazan crystals were dissolved by adding 800 µL dimethyl sulfoxide and the optical density was measured at 370 nm using Multiskan SkyHigh Microplate Spectrophotometer (Thermo-Fischer Scientific, India). OD values of control scaffolds without cells were subtracted from all the group.

2.5.3 Collagen quantification

The total collagen secreted by L929 was quantified in cell lysate using saturated picric acid solution with 0.1% Direct red dye 80 (Sirius red solution) as mentioned in literature [20]. In this assay, sulphonated acid side chain of Sirius red dye binds with basic amino acid side group of collagen. To perform this assay, the cells were cultured on scaffold for 7 days for L929 cells and 14 days for ADSC. The meshes were dipped in 1 ml autoclaved water containing 0.2% Triton X-100 for 10 min and was freeze thawed for 30 min each followed by centrifugation at 4 ^{o}C at 2500 rpm for 10 min. Then 100 µL of cell lysate is mixed with 900 µL of Sirius red solution for 30 min. The mixture was centrifuged for 10 min at 14000 rpm. The supernatant was removed without disturbing the pellet. The extra unbound dye was removed using tissue paper. To the pellet, 500 µL of 0.5N NaOH was added and then vortexed for 10 min. The optical density was measured at 550 nm using Multiskan SkyHigh Microplate Spectrophotometer (Thermo-Fischer Scientific, India).

2.5.4 Cell adhesion imaging

Imaging of cells on the mesh were done using spinning disc confocal microscopy (Yokogawa Electric Corporation, CSU-X1), by staining the cells through a fluorescent dye. Cell seeded meshes were washed with PBS followed by fixing the cells with 4% paraformaldehyde for 2 hrs. The cells fixed on the meshes were washed with PBS followed by permeabilizing cells with 0.2% Triton-X 100 for 10 min. The meshes was washed with PBS then dipped in 2 units/ml of FITC-phallodin stain to stain actin filaments at 4 ^{o}C for 6 hrs. The meshes was washed again with PBS to remove extra FITC-phallodin stain. To stain nucleus, the scaffolds

was dipped in 10 µg/ml of DAPI stain at room temperature for 10 min. The scaffolds was washed again with PBS and then imaged. The images were processed using Zen software (Zeiss).

2.6 In-vitro antibacterial assessment of scaffold

2.6.1 In-vitro bacterial adhesion assessment on scaffold

1 ml of bacterias (*E. coli* K12 or *S. aureus* MTCC 96) at 10^4 CFU/ml in LB broth was added to the scaffold in 24 well plate and was incubated at 37 ^oC for 1 hr and 2 hrs. Later, the scaffold was dipped in 1ml PBS, sonicated for 10 min, vortexed for 1 min to detach the adhered bacterias and was diluted with PBS. After diluting several times, the bacteria were grown on agar plate and the colony forming units per ml was counted. Schematic diagram of bacterial adhesion assessment on scaffold is given in figure 2.

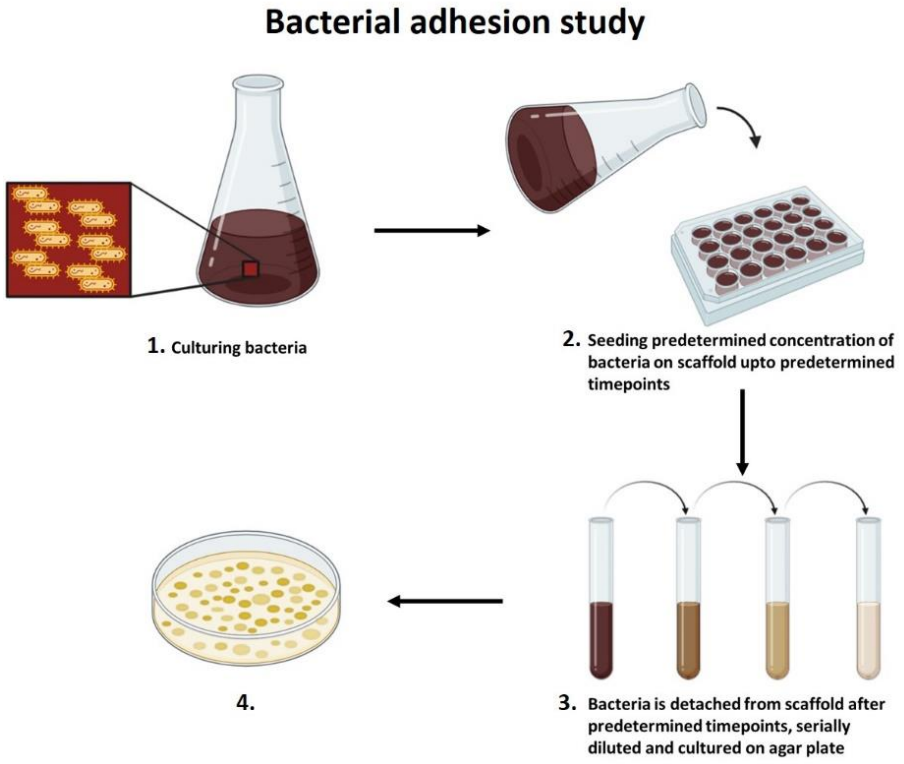

Figure 1: Schematic diagram to assess bacterial adhesion on mesh.

2.6.2 Biofilm Formation on the Scaffold

Biofilm formation on the scaffold was quantified by the tissue culture plate method. Scaffolds were placed in LB broth for 12 hrs and 24 hrs containing 10^4 CFU/ml bacteria. Later, the bacterias on the scaffolds were fixed using glutaraldehyde (2.5%) at 4 ^oC for 30 min and

dried at 60 °C for 1 hr. The biofilms were stained using crystal violet (500 µL, 0.1%) solution at room temperature for 20 min, followed by rinsing with PBS and drying at 37 °C. Stained biofilms on the scaffold were dissolved in 500 µL of 2% acetic acid for 15 min under gentle agitation. The OD at 492 nm was measured using a microplate spectrophotometer.

2.7 Statistical analysis

Datas represented in this article is the result of at-least triplicates of every experiment, expressed as mean ± standard deviation and analysed using one-way analysis of variance (ANOVA). Significance difference was calculated using tukey's test and are represented as *, ** and *** for $P < 0.05$, 0.01 and 0.001.

3 Results

3.1 Mesh fabrication

PCL and PEGC were blended and electrospun (given in table 1). Along with polymer, ZnO nanoparticles were added. SEM images and the fiber size distribution of the commercial mesh, nanoparticle and nanofiber meshes is shown in figure 2. Table 2 lists the fiber diameter of the meshes which is in the range of 0.682 to 0.902 µm. The diameter of the commercially available mesh that was used to treat prolapse is 145 ±8.27 µm. Solution composition and electrospinning parameters play a vital role in fiber diameter distribution of nanofiber diameter. As evident from figure 2C, D, E and F, addition of ZnO increased the nanofiber diameter.

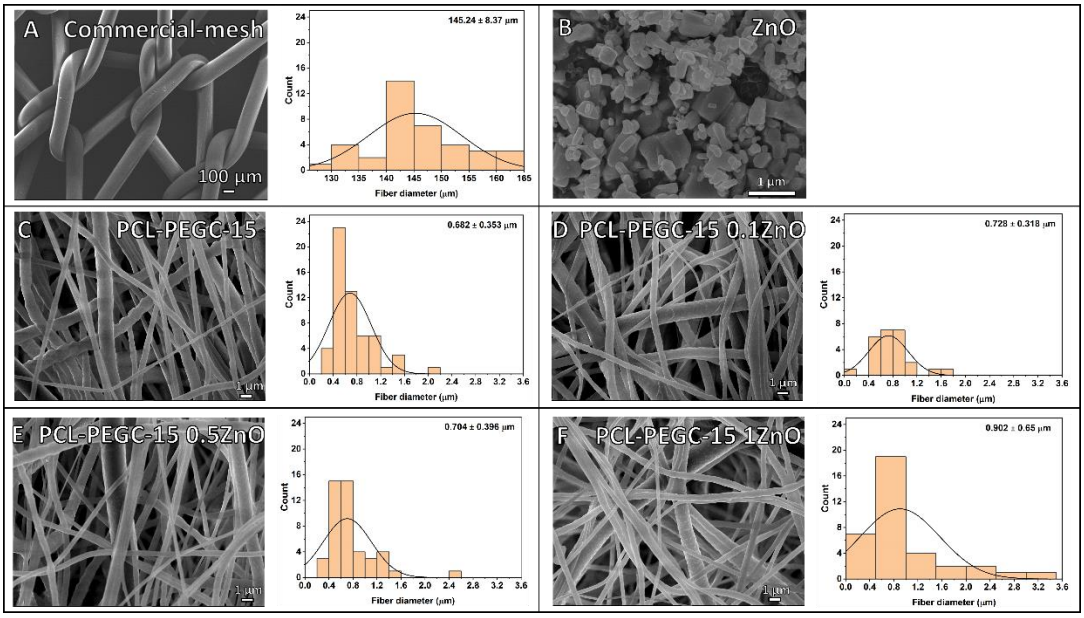

Figure 2: SEM images and fiber size distribution of A) commercial mesh, B) ZnO nanoparticle, C) PCL-PEGC-15, D) PCL-PEGC-15 0.1 ZnO, E) PCL-PEGC-15 0.5 ZnO and F) PCL-PEGC-15 1ZnO nanofiber mesh. Solution composition and electrospinning parameters play a vital role in fiber diameter distribution. Addition of ZnO increased the fiber diameter of the nanofibers**.**

Table 2: Fiber diameters of commercial mesh and PCL-PEGC nanofibers

Sl.no	**Sample code**	**Fiber diameter (µm)**
1	Commercial mesh	145.0±8.270
2	PCL-PEGC-15	0.682±0.353
3	PCL-PEGC-15 0.1ZnO	0.728±0.318
4	PCL-PEGC-15 0.5ZnO	0.704±0.396
5	PCL-PEGC-15 1ZnO	0.902±0.650

3.2 Mesh characterization

3.2.1 Mechanical property evaluation

Optimisation was done based on (i) addition of zinc oxide, (ii) gamma sterilization, and (iii) degradation. The mechanical design criteria of the nanofibrous mesh required to optimised are the minimum ultimate strength- 1MPa and strain 0.7 mm/mm and the range of modulus to be maintained is 5MPa to 11 MPa.

The polymer concentration of 15% is chosen based on the initial pilot investigation on the effect of electrospinning solution concentration on the mechanical property of the nanofibrous mesh. Nanofibrous mesh made out of 20% polymer solution did not meet the mechanical design criteria as the modulus of the mesh fell below 5 MPa. Nanofibrous mesh made out of 10% and 15% polymer solution met the mechanical design criterion but as the mesh degrades there is a high chance of lowering of strain at break. Mesh made of 10% polymer solution has higher chance of loosing strain at break faster than the mesh made out of 15% polymer solution. Additionally, the manufacturing duration for mesh made out of 15% polymer solution will be shorter making polymer concentration of 15% more ideal.

The mechanical property of mesh upon ZnO addition and stress vs strain curves is given in figure 3 A-D and 4 (A-D).

3.2.1.1 Before γ-irradiation:

Before ZnO addition: Without ZnO addition, the ultimate tensile strength (UTS) of PCL-PEGC-15 mesh is 4.5±0.4 MPa i.e., 4.5x higher than the design criteria (1 MPa) before degradation. After 28 days degradation, slightly dropped to 4.0±0.5 MPa but the values are still above the design criteria of 1 MPa. Similarly, strain at break slightly dropped from 2.21±0.16 to 1.89±0.37 mm/mm after 28 days degradation, which is well below the design criteria of 0.7 mm/mm, the required value for an acceptable product. The modulus of PCL-PEGC-15 (without ZnO) mesh before and after 8 days of degradation was 5.2±0.1 MPa and 5.9±0.9 MPa which is within the desired range of the modulus (i.e., 5 to 11 MPa). PCL-PEGC-15 mesh's mechanical properties did not get significantly affected by degradation. All the values conformed to design criteria.

After ZnO addition before degradation: Upon ZnO addition, the UTS of the meshes before degradation were 1.8x to 2.3x times (i.e., at 0.1 wt% ZnO- 2.3±0.1 MPa, at 0.5 wt% ZnO- 1.8±0.1 MPa and at 1 wt% ZnO- 2.0±0.2 MPa) above the design criteria of 1MPa, the strain at break at 0.1 wt% ZnO- 1.53±0.06 mm/mm, at 0.5 wt% ZnO- 1.63±0.15 mm/mm and at 1 wt% ZnO- 1.68±0.05 mm/mm is above the design criteria and the modulus at 0.1 wt% ZnO- 4.1±0.2 MPa, at 0.5 wt% ZnO- 3.9±0.2 MPa and at 1 wt% ZnO- 3.4±0.6 MPa which below the design criteria range. Addition of ZnO significantly reduced the UTS ($P<0.001$), strain at break ($P<0.01$) and modulus ($P<0.05$). The meshes containing ZnO conformed to design criteria of UTS and strain at break but not the modulus. This could be due to reduction in crystalline domains of the mesh upon ZnO addition.

After ZnO addition after degradation: After 28 days of degradation, the UTS of the meshes were 2.2x to 2.4x times (i.e., at 0.1 wt% ZnO- 2.4±0.1 MPa, at 0.5 wt% ZnO- 2.2±0.1 MPa and at 1 wt% ZnO- 2.3±0.2 MPa) above the design criteria of 1MPa, the strain at break at 0.1 wt% ZnO- 1.30±0.09 mm/mm, at 0.5 wt% ZnO- 1.33±0.01 mm/mm and at 1 wt% ZnO- 1.24±0.10 mm/mm is above the design criteria and the modulus at 0.1 wt% ZnO- 5.9±0.7 MPa, at 0.5 wt% ZnO- 6.1±1.3 MPa and at 1 wt% ZnO- 6.1±1.3 MPa. All the meshes after degradation, conformed to the design criteria. The change in mechanical properties in ZnO concentration dependent. At 0.1 wt% ZnO, there was no significant change in UTS and strain

at break after degradation but modulus increased insignificantly. At 0.5 wt% ZnO, there was significant ($P<0.01$) increase in UTS, significant ($P<0.05$) decrease in strain at break and significant ($P<0.01$) increase in modulus after degradation. At 1 wt% ZnO, there was no significant change in UTS after degradation and strain at break decreased ($P<0.01$) significantly but modulus increased but not significantly. After 28 days degradation, all the meshes conformed to design criteria. Addition of ZnO decreased the crystalline domains but upon degradation, as the amorphous domain degraded, the presence of crystalline offered brittleness to the mesh.

3.2.1.2 After γ-irradiation:

Before ZnO addition, before degradation and after γ-irradiation: γ-irradiation had an impact on UTS and strain at break of PCL-PEGC-15 mesh only. Γ-irradiation before degradation, significantly ($P<0.001$) reduced the UTS from 4.5±0.4Mpa to 1.6±0.2Mpa, significantly ($P<0.01$) reduced the strain at break from 2.21±0.16 mm/mm to 1.3±0.00 mm/mm and decreased the modulus but not significantly from 5.2±0.1 Mpa to 4.8 to 0.4 Mpa. This is due to chain scission of crystalline domain reducing the UTS of the mesh and conversion of amorphous domain to crystalline domain reducing the strain at break and thereby keeping the modulus constant before degradation. All the values of the mesh conformed to the design criteria before degradation

Before ZnO addition, after degradation and after γ-irradiation: After 28 days degradation, the UTS increased but not significantly to 1.8±0.3 MPa but the values are still above the design criteria of 1 MPa. However, the strain at break after 28 days degradation reduced significantly ($P<0.001$) from 1.3±0.00 mm/mm to 0.58±0.04 mm/mm, which is below the design criteria of 0.7 mm/mm, and the modulus of PCL-PEGC-15 (without ZnO) mesh significantly ($P<0.01$) increased to 14.4±1.4 MPa. This is due to degradation of amorphous domain from the mesh and the mesh became stiffer due to the presence of crystalline domains.

After ZnO addition, before degradation and after γ-irradiation: Upon ZnO addition, the UTS of the meshes before degradation were 1.8x to 2.7x times (i.e., at 0.1 wt% ZnO- 2.7±0.6 MPa, at 0.5 wt% ZnO- 1.8±0.1 MPa and at 1 wt% ZnO- 1.8±0.0 MPa) above the design criteria of 1MPa, the strain at break at 0.1 wt% ZnO- 1.51±0.05 mm/mm, at 0.5 wt% ZnO- 1.46±0.11 mm/mm and at 1 wt% ZnO- 1.32±0.16 mm/mm is above the design criteria and the modulus

at 0.1 wt% ZnO- 4.7±1.8 MPa, at 0.5 wt% ZnO- 3.7±0.9 MPa and at 1 wt% ZnO- 3.9±0.2 MPa which is slightly below the design criteria range. ZnO behaving like an absorption center prevented γ-irradiation from affect the meshes containing ZnO. The electrospinning parameter i.e., higher flowrate and higher concentration of polymer solution (15 wt%) prevented ZnO from agglomerating leading to the proper dispersion of ZnO in the mesh compared to meshes prepared with lower concentration of polymer solution (15 wt%). Presence of varying concentration of ZnO (0.1, 0.5 and 1 wt% ZnO) did not significantly affect the mechanical properties between the meshes after γ-irradiation.

After ZnO addition, after degradation and after γ-irradiation: After 28 days of degradation, the UTS of the meshes were 2.2x to 2.4x times (i.e., at 0.1 wt% ZnO- 2.0±0.3 MPa, at 0.5 wt% ZnO- 1.8±0.1 MPa and at 1 wt% ZnO- 1.7±0.1 MPa) above the design criteria of 1MPa, the strain at break at 0.1 wt% ZnO- 0.75±0.13 mm/mm, at 0.5 wt% ZnO- 1.00±0.18 mm/mm and at 1 wt% ZnO- 0.73±0.23 mm/mm is above the design criteria and the modulus at 0.1 wt% ZnO- 12.3±0.8 MPa, at 0.5 wt% ZnO- 6.8±1.1 MPa and at 1 wt% ZnO- 8.0±0.0 MPa. The change in mechanical properties in ZnO concentration dependent. At 0.1 wt% ZnO, there was no significant change in UTS after degradation but strain at break significantly decreased ($P<0.001$) and modulus increased ($P<0.01$). Similarly, at 0.5 wt% ZnO, there was no significant change in UTS after degradation but strain at break significantly decreased ($P<0.05$) and modulus increased ($P<0.05$). At 1 wt% ZnO, there was no significant change in UTS after degradation and strain at break decreased but not significantly but modulus increased significantly ($P<0.01$). Even though proper dispersion of ZnO acted as γ-rays absorption center, the partial conversion of crystalline domains to amorphous domain reduced with increasing ZnO concentration. As the mesh degraded, UTS of the meshes remained constant, strain at break impacted only for mesh containing 0.1 wt% and 0.5 wt% ZnO and also impacted modulus of all the meshes. After 28 days degradation all the meshes conformed to the design criteria.

UTS of meshes containing varying ZnO prepared with 15 wt% of polymer concentration, did not get affected with γ-irradiation and degradation meaning these meshes will have same strength but the strain and modulus got affected significantly at the end of 28 days degradation and conforming to the design criteria. Hence, hereafter PCL-PEGC- 15 xZnO

(were x= 0, 0.1, 0.5 and 1 wt% ZnO w.r.t PCL) γ-irradiated meshes were used further for mesh characterization and *in-vitro* studies.

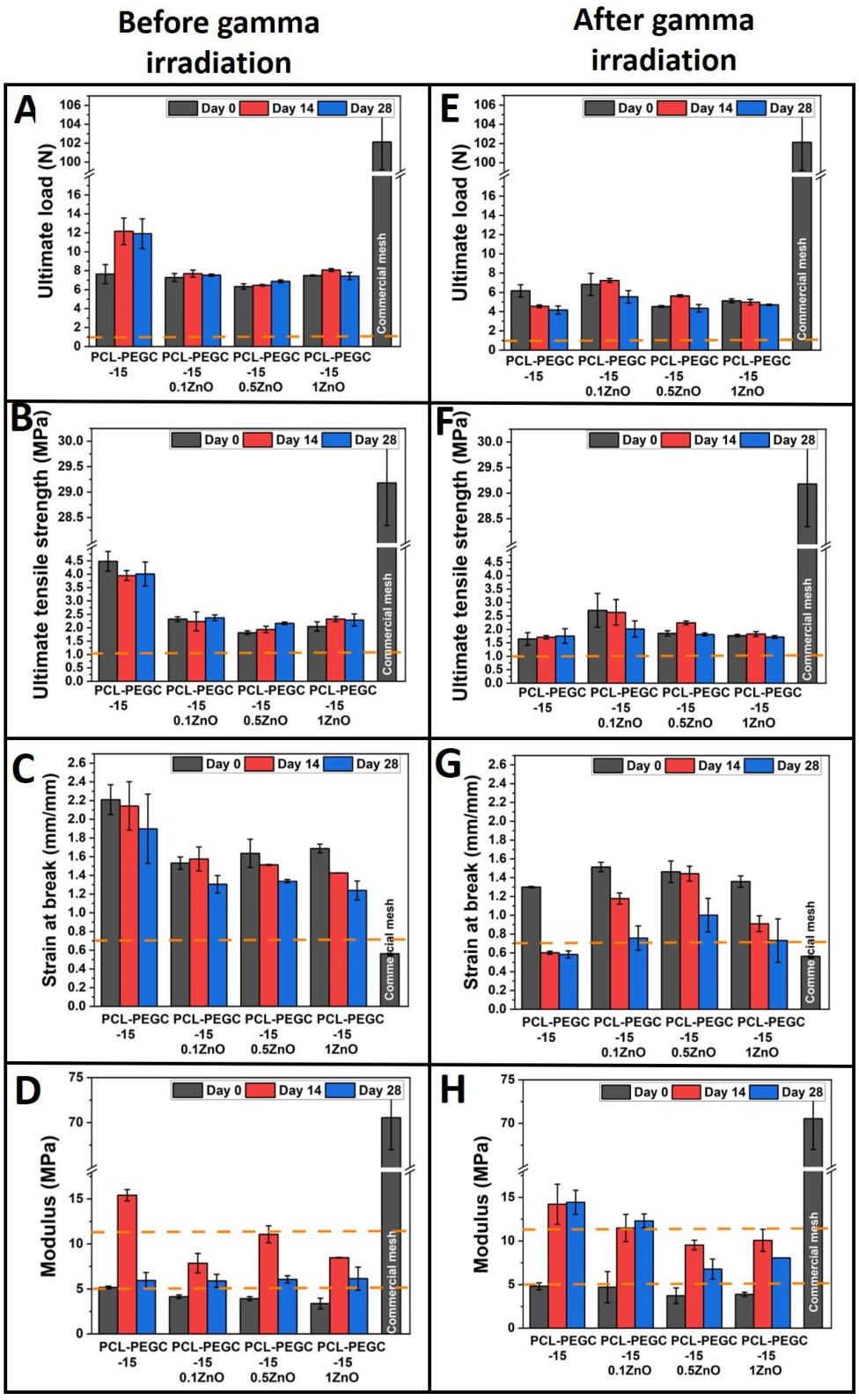

Figure 3: Mechanical property of meshes upon degradation without (A-D) and with (E-H) γ-irradiation. (A, E) Maximum load, (B, F) maximum tensile strength, (C, G) strain at break and

(D, H) modulus of PCL-PEGC-15 xZnO (were x=0, 0.1, 0.5 and 1 wt% of ZnO w.r.t PCL) meshes at day 0, day 14 and day 28 degradation time points.

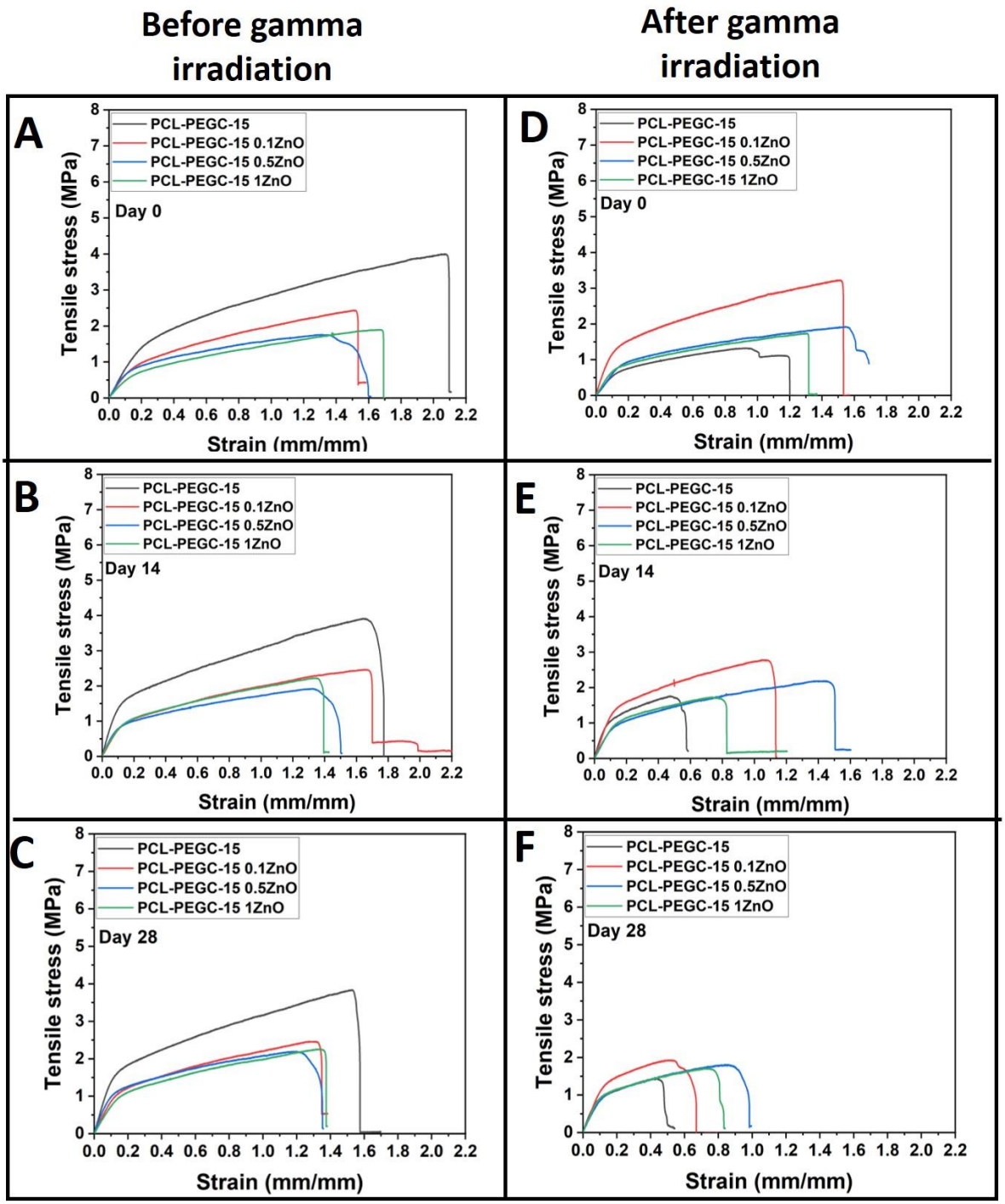

Figure 4: Stress vs strain curves of PCL-PEGC-15 xZnO (where x=0, 0.1, 0.5 and 1) meshes upon degradation at A) day0, B) day14 and C) day28 before and after gamma irradiation.

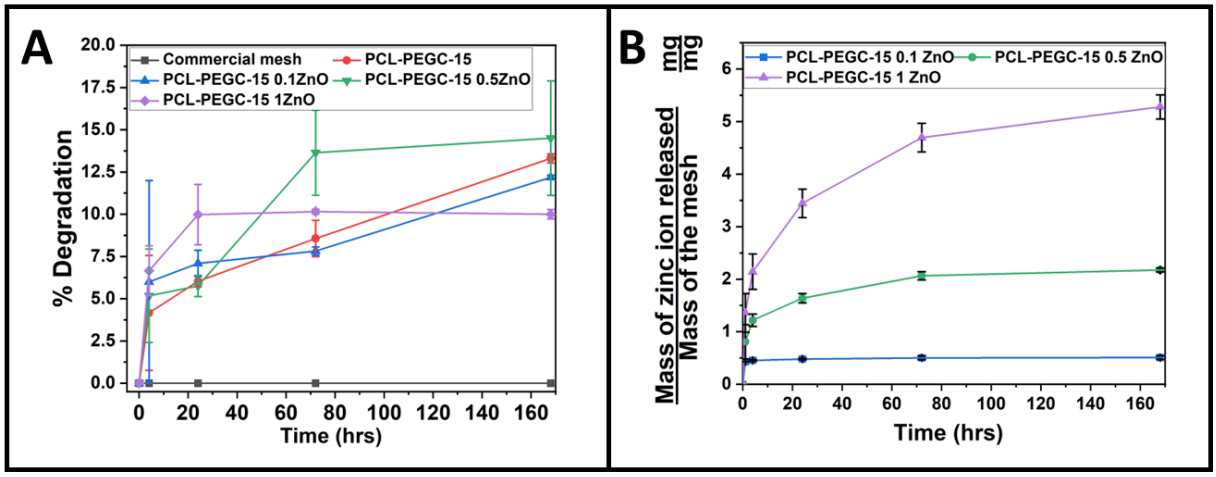

Figure 4: A) Degradation and B) zinc ion release from PCL-PEGC-15 xZnO (where x=0, 0.1, 0.5 and 1) meshes.

3.2.2 Mesh degradation

The degradation profile of mesh (figure 4 A) shows that PCL-PEGC-15 xZnO (where x=0, 0.1, 0.5 and 1) meshes showed similar degradation behaviour. 10% of mesh degraded at day 7.

3.2.3 Ion release profile

Zinc ion release profile from PCL-PEGC-15 xZnO (were x=0, 0.1, 0.5 and 1 wt% of ZnO w.r.t PCL) mesh (figure 4 B) shows that with increasing ZnO nanoparticle in the mesh, zinc ion release was higher. All the meshes showed burst release of zinc ion initially.

3.3 Evaluation of mesh performance *in-vitro*

In this study, the meshes were tested for biocompatibility and collagen production efficacy using L929 to find out the best suitable composition for pelvic floor repair which was subsequently tested with adipose derived stem cells. The experiments were performed on γ-irradiated meshes and the results of MTT assay, collagen assay on day 7 and confocal images of cells on the scaffold on day 7 is given in figure 5.

Biocompatibility evaluation using L929: The commercial mesh, PCL-PEGC-15 and PCL-PEGC-15 0.1 ZnO meshes supported cell growth and collagen production. With further increase of ZnO loading, higher ZnO release became toxic for L929 growth because of higher reactive oxygen species produced by ZnO [29]. The actin and nucleus staining of L929 seeded on mesh as shown in figure 5D-F and 5D'-F' reconfirmed the biocompatibility result obtained

from MTT assay. Out of commercial mesh, PCL-PEGC-15 and PCL-PEGC-15 0.1ZnO meshes, PCL-PEGC-15 0.1ZnO mesh supported higher collagen production *in-vitro*.

Collagen production: Collagen synthesis occurs in the fibroblast both intercellularly and extracellularly [31]. The total collagen assay as shown in figure 5B shows the effect of mesh on collagen synthesis of fibroblast. In comparison with the commercial mesh, PCL-PEGC-15 and PCL-PEGC-15 0.1ZnO meshes supported collagen production, out of which PCL-PEGC-15 0.1ZnO mesh significantly enhanced collagen production of L929 fibroblast.

Haemocompatibility: Haemocompatibility assay performed as per ASTM F756-17 as shown in figure 5C confirmed that, all the meshes i.e., both commercial and PCL-PEGC-15 xZnO (were x=0, 0.1, 0.5 and 1 wt% of ZnO w.r.t PCL) meshes are non-haemolytic and will not cause any adverse side reaction upon implantation *in-vivo*.

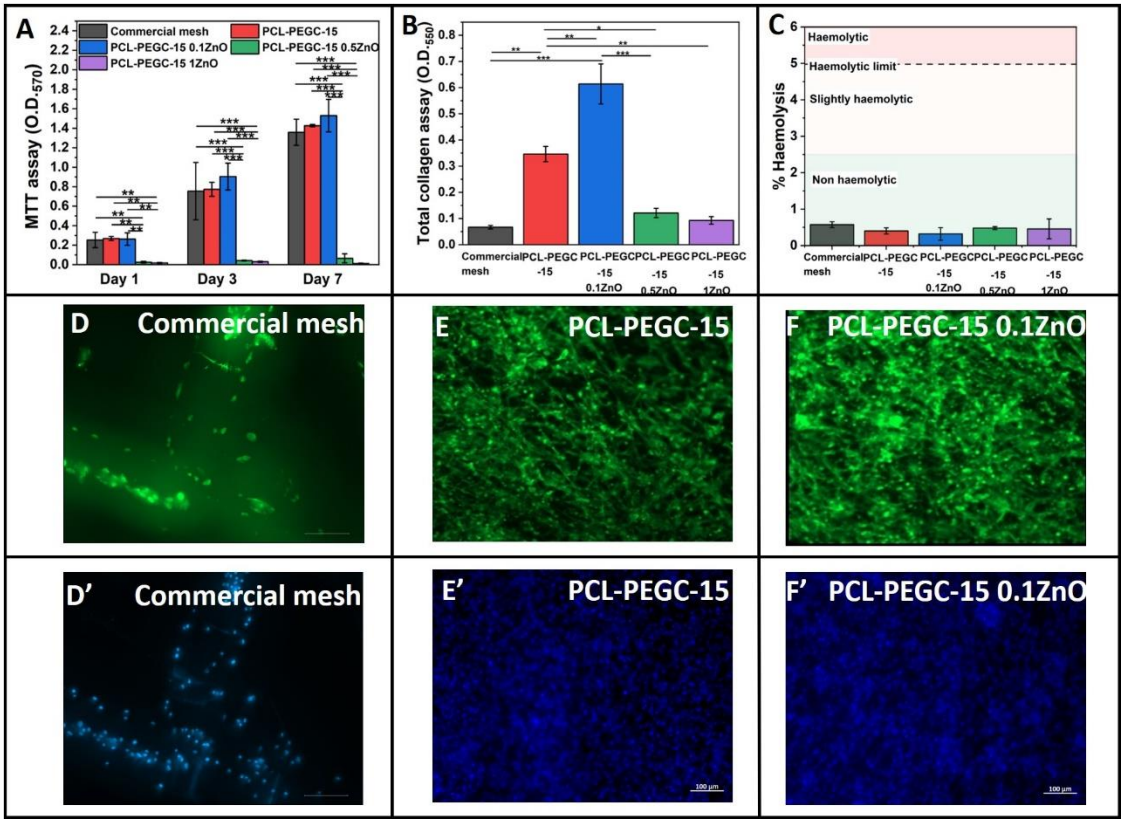

Figure 5: A) MTT assay, B) total collagen assay at Day 7, C) haemocompatibility assay, D-F) FITC stained actin of the L929 adhered on the meshes on day 7 and D'-F') DAPI stained nucleus of the L929 adhered on the meshes on day 7. The mesh formulations PCL-PEGC-15 and PCL-PEGC-15 0.1 ZnO supported cell growth and collagen production and collagen

production was higher for PCL-PEGC-15 0.1 ZnO meshes. The commercial mesh was biocompatible but did not support collagen production *in-vitro*.

3.4 Antibacterial evaluation of the mesh

The antibacterial efficacy of the scaffold was analyzed by using *E. coli* and *S. aureus* as the model bacteria. The commercial meshes and electrospun meshes was placed in an environment that supported bacterial proliferation. The results of bacterial adhesion and biofilm formation is given in figure 6.

Bacterial adhesion: The bacterial adhesion study was performed on the commercial meshes and nanofiber meshes at 1 hr and 2 hrs using *E. coli* and *S. aureus* as shown in figure 6 A and B. Gram negative bacteria *E. coli* at 1 hr had significantly higher adhesion to commercial mesh than nanofiber meshes. At 2 hrs, there is 2 log reduction ($P<0.001$) in bacterial adhesion on the nanofiber meshes in comparison with commercial mesh. Gram positive bacteria *S. aureus* at 1 hr had 1 log reduction in bacterial adhesion for the nanofiber meshes containing 0.5 wt% and 1 wt% ZnO i.e., PCL-PEGC-15 0.5ZnO and PCL-PEGC-15 1ZnO meshes. At 2 hrs, there is 2 log reduction ($P<0.001$) in bacterial adhesion on PCL-PEGC-15 and PCL-PEGC-15 0.1ZnO meshes and >2 log reduction on PCL-PEGC-15 0.5ZnO and PCL-PEGC-15 1ZnO meshes in comparison with commercial meshes.

Biofilm formation: Biofilm formation assay was performed on the commercial meshes and nanofiber meshes at 12 hr and 24 hrs using *E. coli* and *S. aureus* as shown in figure 10 C. Biofilm of gram negative bacteria *E. coli* on commercial mesh and nanofiber meshes at 12 hrs were not significantly different. But at 24 hrs, there is no significant difference between commercial mesh and nanofiber meshes containing 0, 0.1 wt% and 0.5 wt% ZnO. However, there is a significant ($P<0.05$) reduction of biofilm on PCL-PEGC-15 1ZnO mesh with respect to commercial mesh. Biofilm of gram positive bacteria *S. aureus* on nanofiber meshes at 12 hrs and 24 hrs were significantly lower than commercial mesh.

The antibacterial action of ZnO is due to the positively charged nanoparticle onto the negatively charged bacterial membrane causing membrane instability and also by release of reactive oxygen species [13], [14].

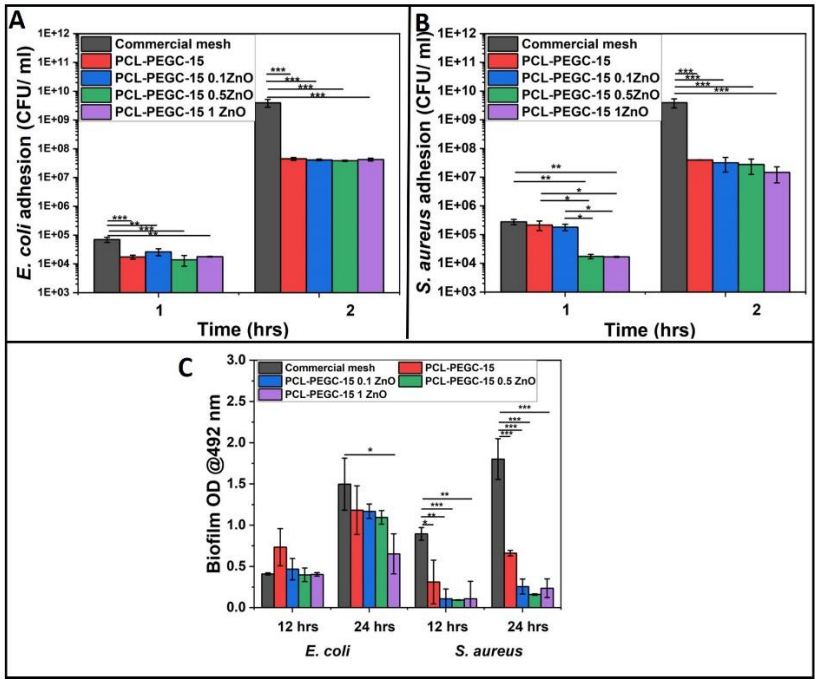

Figure 6: Bacterial adhesion study: colony forming units (CFU) of A) *E. coli,* B) *S. aureus* adhesion and C) biofilm formation on meshes. At 2 hrs timepoint, all the meshes exhibited 2 log reduction in bacterial adhesion in comparison with commercial mesh. Biofilm formation on the meshes were lower in comparison to commercial mesh. Meshes containing ZnO reduced *S. aureus* biofilm than *E. coli* biofilm.

4 Discussion

POP is a common gynaecological disorder observed in menopausal women. Hormonal changes in post-menopausal women plays a key role in altering the ECM of the pelvic floor support structures. Proteins in ECM consists of collagen, elastin, fibrillin, fibronectin, laminin, and proteoglycan [15]. Collagen and elastin contribute towards the mechanical property of the vaginal wall [15]. The vaginal wall premenopause is composed of collagen (84%) and elastin (13%). The premenopausal women have higher ratio of collagen I/(III+V) and lower for menopausal and women with prolapse due to upregulation of matrix metalloproteinases [16]. This is clearly evident from the mechanical property of vaginal tissue pre and post prolapse as reported in literature [11]. As the ratio of collagen, I/(III+V) and elastin content dropped the maximum tensile strength, elongation reduced and increased the modulus (stiffness) of the tissue. Thus, compromised the mechanical property of vaginal wall.

Designing biodegradable mesh for pelvic floor should overcome the disadvantages of biological grafts and non-resorbable mesh. The key factor that was missed out in earlier design is the mismatch of mechanical properties. The average weight of uterus is between 50 to 80 g [17] and average weight of bladder based on ultrasound evaluation is around 67 g [18]. Therefore, roughly the mesh should withstand minimum 1N load. Based on the mechanical property of the vagina [11], the mesh should possess minimum of ultimate tensile strength around 1MPa [11] and modulus in the range of 5 to 11 MPa [11]. Modulus determines the stiffness of the material. Higher the modulus, higher the stiffness. For pelvic floor repair, higher stiffness (>11 MPa) mesh is not desirable and will cause discomfort to the patients. Mechanical properties in the meshes is achieved by fine tuning the composition and the electrospinning parameters of PCL, PEGC and ZnO. In this study, the minimum strain at break (mm/mm) is fixed at 0.7, higher than the strain at break of commercial mesh. Further higher strain in a degradable mesh will result in tissue remodelling in sagged mesh thereby herniation. Therefore, the composition of the electrospinning solution and electrospinning parameter is optimised as per the mechanical design criteria discussed above.

Before implanting medical devices inside human body, it is necessary to sterilize either using gamma-irradiation, ethylene oxide, steam (autoclaving), dry heat or vaporized hydrogen peroxide to eliminate all the pathogens. Since the nanofiber mesh is thermosensitive, low temperature sterilization techniques like gamma -irradiation, ethylene oxide or vaporized hydrogen peroxide are highly preferable. γ-irradiation has little impact on material's property, this technique is used in our work because the cell's response *in-vitro* has no effect in comparison with other sterilization technique [19]. When a polymer is irradiated, three different process takes place: (i) chain scission, crosslinking or grafting as the polymer backbone initiates free radical process. The strength of polymer increased might be due to the hydroxyl group in (i) unreacted citric acid and PEG, (ii) between unreacted PEG and (iii) PEGC, PEGC and citric acid has further crosslinked [20], [21]. Despite gamma-irradiation, the mechanical properties of all the meshes were altered but they were within the mechanical design criteria of the biodegradable mesh.

Meshes upon *in-vitro* evaluation showed biocompatibility and haemocompatibility. Collagen synthesis is an essential part in pelvic floor repair. Citric acid grafting in PEG improved

the collagen synthesis of the micro-nanofiber meshes [22]. Addition of ZnO further enhanced the collagen synthesis [23], [24]

Formulating mesh composition that not only is biocompatible but also antibacterial is essential to prevent mesh related infections. Commercial mesh does not have any functional group that either prevent bacterial adhesion or kill bacteria upon contact. Surface chemistry, hydrophobicity and porosity of the surface plays a critical role in bacterial adhesion. The commercial mesh is made of polypropylene and its hydrophobic surface made it favourable for bacterial adhesion [25]. Presence of PEG in PEGC and ZnO provided passive antibacterial activity by preventing the adhesion of bacterias and better antibacterial effect against *S. aureus* than *E. coli*. Amongst all the micro-nanofiber meshes, PCL-PEGC-15 0.1ZnO mesh supported biocompatibility, collagen production ability and bacteriostatic ability essential for successful pelvic floor repair.

5 Impact of the research in the advancement of knowledge or benefit to mankind

This research addresses global problem faced by menopausal women by developing a mesh that is exclusively designed for the treatment of pelvic floor issues like prolapse and incontinence. Currently there is no product in the market that can be used to treat prolapse and incontinence as the already existing products were banned. In India, around 4.56 crore women have severe prolapse and incontinence. This research will address the market need. This work gained recognition through various grants like BIRAC-PACE-AIR and WRCB and was showcased in G-20 RIIG Summit and Research Minister's meeting, IITBombay, Mumbai, Maharashtra, July 6, 2023. This research will be translated and will be introduced in Indian market.

6 Conclusion

Biocompatible, biodegradable, bacteriostatic and soft meshes were prepared out of PCL, PEGC and ZnO through electrospinning technique for pelvic floor repair. All the micro-nanofiber meshes matched the mechanical design criteria for pelvic floor. Among various PCL-PEGC-15 xZnO (were x=0, 0.1, 0.5 and 1 wt% of ZnO w.r.t PCL) meshes, PCL-PEGC-15 0.1ZnO mesh not only supported cell growth and enhanced collagen production but also offered bacteriostatic effect than the commercial mesh. The mechanical properties of PCL-PEGC-15

0.1ZnO mesh improved with ECM formation. Therefore, PCL-PEGC-15 0.1ZnO meshes is more suitable for its application in pelvic floor repair.

7 Reference

[1] Giarenis, I. and Robinson, D., 2014. Prevention and management of pelvic organ prolapse. *F1000prime reports*, *6*.

[2] Willis, O. (2018) *'I wish someone had told me': Why we need to talk about women's pelvic floors*, *ABC News*. ABC News. Available at: https://www.abc.net.au/news/health/2018-07-07/ why-we-need-to-talk-about-womens-pelvic-floor-health /9945920 (Accessed: March 9, 2023).

[3] *What is pelvic organ prolapse and how common is it?* (2019) *Queensland Health*. The State of Queensland. Available at: https://www.health.qld.gov.au/news-events/news/what-is-pelvic-organ-prolapse-symptoms-treatment-childbirth-womens-health (Accessed: March 9, 2023).

[4] Subramanian, D., Szwarcensztein, K., Mauskopf, J.A. and Slack, M.C., 2009. Rate, type, and cost of pelvic organ prolapse surgery in Germany, France, and England. *European Journal of Obstetrics & Gynecology and Reproductive Biology*, *144*(2), pp.177-181.

[5] Mancuso, E., Downey, C., Doxford-Hook, E., Bryant, M.G. and Culmer, P., 2020. The use of polymeric meshes for pelvic organ prolapse: Current concepts, challenges, and future perspectives. *Journal of Biomedical Materials Research Part B: Applied Biomaterials*, *108*(3), pp.771-789.

[6] Magalhaes, R.S. and Atala, A., 2019. Scaffolds for vaginal tissue reconstruction. In *Handbook of Tissue Engineering Scaffolds: Volume Two* (pp. 317-332). Woodhead Publishing.

[7] Yuan, M., Hu, M., Dai, F., Fan, Y., Deng, Z., Deng, H. and Cheng, Y., 2021. Application of synthetic and natural polymers in surgical mesh for pelvic floor reconstruction. *Materials & Design*, *209*, p.109984.

[8] Commissioner (2019) *FDA takes action to protect women's health, orders manufacturers of surgical mesh intended for transvaginal repair of pelvic organ prolapse to stop selling all devices*, *U.S. Food and Drug Administration*. FDA. Available at: https://www.fda.gov/news-events/press-announcements/fda-takes-action-protect-womens-health-orders-manufacturers-surgical-mesh-intended-transvaginal (Accessed: March 9, 2023).

[9] Badami, A.S., Kreke, M.R., Thompson, M.S., Riffle, J.S. and Goldstein, A.S., 2006. Effect of fiber diameter on spreading, proliferation, and differentiation of osteoblastic cells on electrospun poly (lactic acid) substrates. *Biomaterials*, *27*(4), pp.596-606.

[10] Dykes, N., Karmakar, D. and Hayward, L., 2020. Lightweight transvaginal mesh is associated with lower mesh exposure rates than heavyweight mesh. *International Urogynecology Journal*, *31*, pp.1785-1791.

[11] Lei, L., Song, Y. and Chen, R., 2007. Biomechanical properties of prolapsed vaginal tissue in pre-and postmenopausal women. *International Urogynecology Journal*, *18*, pp.603-607.

[12] Lu, Y., Dong, S., Zhang, P., Liu, X. and Wang, X., 2017. Preparation of a polylactic acid knitting mesh for pelvic floor repair and in vivo evaluation. *Journal of the Mechanical Behavior of Biomedical Materials*, *74*, pp.204-213.

[13] Preethi, A. and Bellare, J.R., 2021. Tailoring scaffolds for orthopedic application with anti-microbial properties: Current scenario and future prospects. *Frontiers in Materials*, *7*, p.594686.

[14] Abdelghafar, A., Yousef, N. and Askoura, M., 2022. Zinc oxide nanoparticles reduce biofilm formation, synergize antibiotics action and attenuate Staphylococcus aureus virulence in host; an important message to clinicians. *BMC microbiology*, *22*(1), pp.1-17.

[15] Saputra, A.N.D., Rizal, D.M., Ayuandari, S. and Pangastuti, N., 2022. The difference in collagen type-1 expression in women with and without pelvic organ prolapse: a systematic review and meta-analysis. *International Urogynecology Journal*, *33*(7), pp.1803-1812.

[16] Abramowitch, S.D., Feola, A., Jallah, Z. and Moalli, P.A., 2009. Tissue mechanics, animal models, and pelvic organ prolapse: a review. *European Journal of Obstetrics & Gynecology and Reproductive Biology*, *144*, pp.S146-S158.

[17] Dutta, D.C., 2003. *Textbook of gynaecology*. New central book agency.

[18] Al-Shaikh, G. and Al-Mandeel, H., 2012. Ultrasound estimated bladder weight in asymptomatic adult females. *Urology Journal*, *9*(3), pp.586-591.

[19] Horakova, J., Klicova, M., Erben, J., Klapstova, A., Novotny, V., Behalek, L. and Chvojka, J., 2020. Impact of various sterilization and disinfection techniques on electrospun poly-ε-caprolactone. *ACS omega*, *5*(15), pp.8885-8892.

[20] Ajji, Z., 2005. Preparation of poly (vinyl alcohol) hydrogels containing citric or succinic acid using gamma radiation. *Radiation Physics and Chemistry*, *74*(1), pp.36-41.

[21] Abu Ghalia, M. and Dahman, Y., 2015. Radiation crosslinking polymerization of poly (vinyl alcohol) and poly (ethylene glycol) with controlled drug release. *Journal of Polymer Research*, *22*, pp.1-9.

[22] Yin, X., Li, Q., Wei, H., Chen, N., Wu, S., Yuan, Y., Liu, B., Chen, C., Bi, H. and Guo, D., 2019. Zinc oxide nanoparticles ameliorate collagen lattice contraction in human tenon fibroblasts. *Archives of biochemistry and biophysics*, *669*, pp.1-10.

[23] Wu, M., Cronin, K. and Crane, J.S., 2018. Biochemistry, collagen synthesis.

[24] Cole, M.A., Quan, T., Voorhees, J.J. and Fisher, G.J., 2018. Extracellular matrix regulation of fibroblast function: redefining our perspective on skin aging. *Journal of cell communication and signaling*, *12*, pp.35-43.

[25] Verhorstert, K.W., Guler, Z., de Boer, L., Riool, M., Roovers, J.P.W. and Zaat, S.A., 2020. In vitro bacterial adhesion and biofilm formation on fully absorbable poly-4-hydroxybutyrate and nonabsorbable polypropylene pelvic floor implants. *ACS Applied Materials & Interfaces*, *12*(48), pp.53646-53653.